Start-Up and Shut-Down Simulation of a Thermal Barrier Coated Gas Turbine Bucket Using CFD Code

Conference Paper · September 2008

DOI: 10.1115/POWER2008-60145

3 authors, including:

Eder Arturo Bautista Pérez

3 PUBLICATIONS **8** CITATIONS

SEE PROFILE

Zdzislaw Mazur

Instituto de Electricidad y Energías limpias.

13 PUBLICATIONS **159** CITATIONS

SEE PROFILE

Proceedings of POWER2008
ASME Power 2008
July 22-24, 2008, Orlando, Florida, USA

POWER2008-60145

START-UP AND SHUT-DOWN SIMULATION OF A THERMAL BARRIER COATED GAS TURBINE BUCKET USING CFD CODE

Alejandro Hernández Rossette, Zdzislaw Mazur C, Rodolfo Muñoz, Eder Bautista

Electrical Research Institute
Av. Reforma 113, Col. Palmira, 62490 Cuernavaca Morelos, México
Tel: 52 777-3623811, Fax: 52 777-3623834
E-mail: ahr@iie.org.mx

ABSTRACT

The unsteady aerodynamics and aerothermics of a first stage gas turbine bucket with thermal barrier coating (TBC) and internal cooling configuration were investigated by application of a three dimensional Navier-Stoke commercial turbomachinery oriented CFD-code. Convection and conduction were modeled for a super alloy blade with TBC. This work is the second part of the paper "Unsteady 3-d conjugated heat transfer simulation of a thermal barrier coated gas turbine bucket", and includes the simulation of shut down cycle.

The CFD simulations were configured with a mesh domain of nozzle and bucket inter-stage using real turbine parameter data as boundary condition (BC) at nozzle inlet. The BC´s were adjusted in accordance with standard start-up and shut-down diagram for a gas turbine from Takahashi work [3]. Additionally a parabolic turbine inlet temperature was set for main gas flow. The problem was launched in a minicluster of 8 HP Workstation. Reasonably good comparisons in the main flow parameters with the manufacturer data were obtained.

The effects of blade TBC surface temperature changes during a start-up and shut-down cycle were simulated using the Spalart-Allmaras turbulence model. A TBC can be used either to reduce the need for blade cooling (by about 36%) increasing the turbine efficiency, while maintaining identical creep life of the substrate; and increase considerably the creep life of the blade while maintaining level of blade cooling (and therefore allowing the blade to operate at lower temperature for an identical turbine entry temperature).

KEYWORDS

CFD, Conjugate heat transfer, Gas turbine blade, Thermal Barrier Coating, Convection and Conduction, Numerical simulation and Temperature Prediction, Transient analysis.

INTRODUCTION

The important research areas related to heat transfer to a gas turbine blade include external and internal heat transfer coefficient predictions, metal temperature distribution, blade cooling methods, rotation effects, and ceramic coatings. External convection depends upon the development of the boundary layer on the blade surface, which is complex phenomenon, and there is considerable uncertainty associated with both numerical predictions and experimental measurements.

Some analysis [21] shows that using TBC and very limited film cooling had predicted that thermal efficiency of up to 60% is attainable if coolant does not mix with the main stream. Losses associated with extensive film cooling, dilution of hot gas with coolant, aerodynamic mixing loss and rotor blade pumping loss are almost completely eliminated in this manner. These developments indicate that ceramic-coated blades with out extensive film cooling are necessary for achieving higher efficiencies

The necessity of close control of the materials surface temperatures can be expressed by the simple rule that blade life

in creep is halved for every 10-15º increase in temperature. Further increase in the thrust to weight ratio of advanced aero engines will require even higher gas-turbine inlet temperatures passing well beyond 1,600ºC.

These high gas turbine temperatures can only be maintained through advanced cooling techniques and the introduction of electro-beam physical vapor deposition (EB-PVD) or thermal barrier coatings (TBCs). The application of the TBCs increases the engine performance by either increasing the gas turbine inlet temperature, or reducing the required air cooling flow which is beneficial from the standpoint of reduction of NOx production and as mean of improving cycle efficiency. Previous works [1] have shown that reducing from 10% to 5% off main-stream air can lead to NOx reductions of nearly 25% while maintaining the same rotor inlet temperature. Alternatively, the life time of the turbine blades can be extended by decreasing the metal temperature. Besides, it is well known that start-up and shut-down cycles affect blade life through thermal fatigue of the structural material, because of variations of thermal loads. The impact of these cycles mainly depends on three dimensional behavior of the blade temperature distribution, which is influenced by inlet gas flow conditions, blade rotation, internal cooling and ejected flow of cooling flow from the blade tip, etc, depending on the time in operation.

The present authors have studied the temperature distribution changes for first stage moving blade in steady state and during a typical start-up cycle. In the first case the temperature prediction shows a protective bucket surface temperature up to 65 K. In the second case when a start-up cycle was simulated the Delta Temperature in the TBC from exterior surface thru bucket surface had a minimum value of 12 K rising up to full load with 87 K.

The main objective of the present paper is to predict the temperature behavior of the first stage TBC Bucket in a start-up and shut down cycle by means of a transient analysis using a multi-block three dimensional Navier-Stokes commercial turbomachinery oriented CFD code. The behavior of TBC depending on time will be discussed and compared with results from previous works [2].

NOMENCLATURE

t , Δt	Time [seconds]
K	Thermal conductivity [W/mK]
TIT	Turbine inlet temperature [K]
Cp	Specific heat [J/Kg-K]
G	Mass Flow Rate (kg/s)
RO	Time of rated operation [seconds]
PI,PO	Time of parallel In and Parallel Off [seconds]
LE,TE	Leading Edge, Trailing Edge
Nr	Rotor Speed [rpm]
P, Po	Static Pressure, Relative Total Pressure [Pa]
y^+	dimensionless wall distance
TBC	Thermal barrier coating
ρ	Density Kg/m^3
Tair	Compressor outlet temperature [K]
Gair	Compressor inlet mass flow [Kg/s]
Pout	Turbine output [Watts]
SA	Spalart-Allmaras turbulence model

DESCRIPTION OF ANALYSIS

Computational method

The numerical scheme solves the 3D (RANS) on general structured non-orthogonal, multi-block grids. The flexibility of the structured grids is greatly enhanced by used of the so called "Full Non Matching Connections", a technique which allows to arbitrarily connect grid blocks of different grid topologies or densities. This permits for instance to independently mesh the solid and fluid domains, the only condition being that the two meshes connect onto a common surface (the blade surface).

The numerical algorithm incorporated in solver is an explicit four stage Runge-Kutta scheme (Jameson and Baker, 1984 [6]). A variety of convergence acceleration techniques are employed, such as implicit residuals smoothing and MultiGrid, Space integration is performed using a second order cell centered finite volume discretization with second and fourth order artificial dissipation. Coarse grid calculations can be carried out in an automatic way during the computation initialization. In the present work the one equation turbulence model Spalart-Allmaras has been chosen.

The Conjugated Heat Transfer (CHT) module included in the solver the conduction equation in the solid parts of the domain. The conduction equation can be seen as the energy equation of the Navier-Stokes system, where all velocities are set to zero. This equation can be numerically solved similarly as the flow equations, with a finite-volume approach, allowing for the use of the same acceleration techniques such as MultiGrid. The CFL time step calculation needs an adaptation, being exclusively based on diffusion. The major advantage of this module is that it permits to eliminate the question of determining appropriate boundary conditions along the blade surface, these conditions being generally unknown. One just needs to specify the temperature of the cooling flow propagating in the inner channels, and the boundary conditions come naturally from the solving of CHT. This module has been extensively validated for gas turbines [5].

Grid

The numerical domain has the same configuration that previous works [2], using a structured multi-block grid. The boundary layer is discretized by several finite volume cells, so that the first cell center in the flow region has a dimensionless wall distance of y^+ approximately of 2 allowing a correct determination of the local heat flux for the coupling condition.

The CFD simulations were configured with a mesh domain including the nozzle and the bucket inter-stage space, in order to accurately predict the fluid parameters at inlet and outlet of bucket. The flow conditions at the inlet of the rotor have been validated with turbine inter-stage parameter data test of gas turbine manufacturer in base load. It would have been possible to perform the simulations separately for the nozzle and the rotor (and then afford denser meshes), but several iterations may have been needed before converging to the right boundary conditions to be applied at the nozzle-rotor interface.

The entire domain is composed by nozzle and bucket rows for the first stage as seen in figure 1. Thirteen radial cooling holes were meshed in the bucket as well as the solid domains for the bucket blade and TBC. Emphasis was put on a high grid quality in order to minimize numerical dissipation, particularly inside the cooling holes and their immediate vicinity.

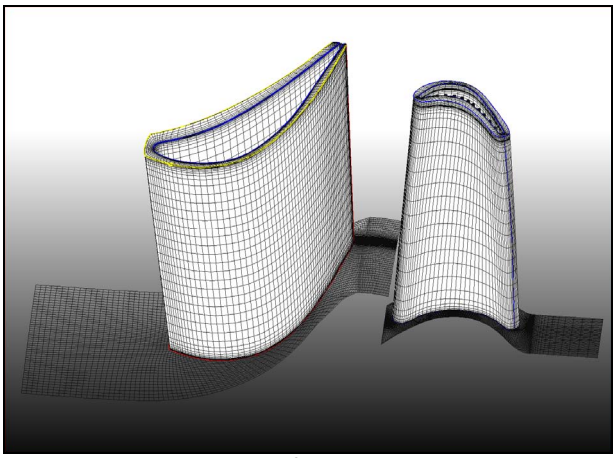

Figure 1. General view of the Nozzle and Bucket blades with cooling holes inside the rotor and fluid mesh.

A multi-block butterfly topology was applied to the cooling holes drastically improving cells orthogonally as shown in Figure 2.

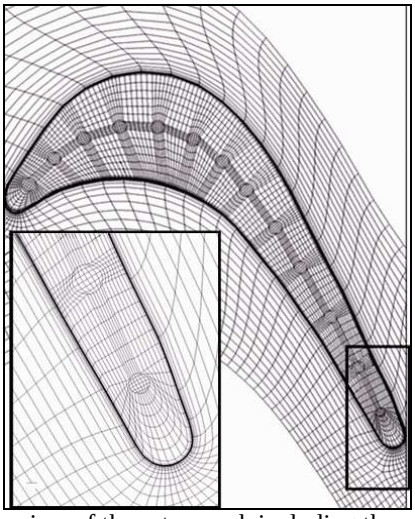

Figure 2. Top view of the rotor mesh including the radial holes, Detail close-up near TE

Boundary conditions

The BC´S imposed to the model are shown in table 3. These values were taken from turbine inter-stage parameter data test of gas turbine manufacturer. According to this diagram there is a non-load operation region before the Parallel In (PI). The load of the GT gradually increases from the PI to the rated load operation (RL) point in the Start-Up curve. An interesting curve is the Turbine Inlet Temperature (TIT), which rapidly increases since Ignition and Crossfire (0 sec) to reach a local maximum; then the temperature decreases, and restarts increasing at the PI point. This is a point of interest since thermal fatigue duty is associated with the start-up process. When the running speed is reached the load operation begins with a more stable TIT rise, up to rated load. The compressor outlet flow and its temperature are also presented in Figure 4 diagram.

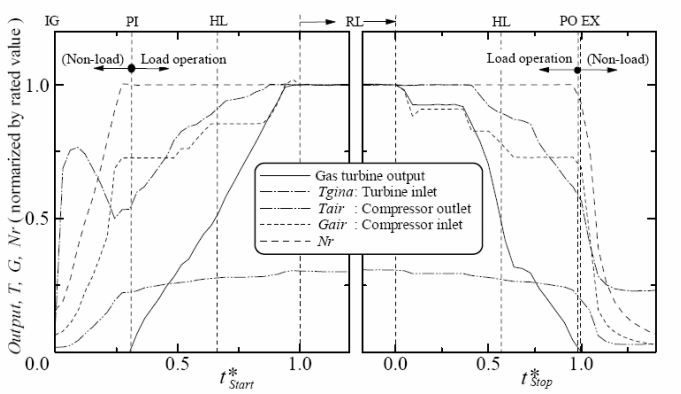

Figure 3. Start-Up and Shut-down Diagram for a GT [3].

The model BC's can be summarized as follows:

- The gas mass flow [G] and TIT, were imposed based on polynomial equations depending on time that correspond with curves of figure 4.
- The TIT at nozzle was assumed as parabolic profile along span height in order to obtain a more realistic temperature distribution along the nozzle and bucket bodies. See Figure 5.
- The compressor outlet flow curve [Gair] was used to obtain the 2% of cooling air mass flow. For a better fit, 5 polynomial sub equations were used for the configuration during Start-Up.
- The air cooling Temperature [Tair] and Outlet Static Pressure [OSP] were calculated both using the TIT Start-Up curve and thermodynamic equations that consider room atmospheric conditions for inlet and outlet of domain, as well as, Outlet Gas Temperature and typical efficiencies for the Compressor and Gas Turbine.
- The air cooling temperature for the bleeding simulation module of the nozzle was also treated in an unsteady way, the temperature being identical for both the nozzle and rotor cooling.
- During CFD simulation the RPM was assumed constant.

The bucket base material is an Inconel 738 LC Superalloy and the TBC is composed of 0.4 mm thick YSZ. Polynomial expressions for thermal conductivity and specific heat for both Inconel 738 LC and TBC have been derived, taking into account the investigated temperature range:

Inconel738LC Thermal Conductivity [W/mK]:

$$K = -1.5331\times10^{-08}T^3 + 4.3688\times10^{-05}T^2 - 2.2064\times10^{-02}T + 14.72$$

TBC-YSZ Thermal Conductivity [W/mK]:

$$K = 8.6072\times10^{-07}T^2 - 1.1651\times10^{-03}T + 1.1708$$

Inconel738LC Specific Heat [J/kg-K]:

$$C_P = -1.42\times10^{-09}T^4 + 4.8269\times10^{-06}T^3 - 5.7607\times10^{-03}T^2 + 3.066T - 99.132$$

TBC-YSZ Specific Heat [J/kg-K]:

$$C_P = 4.4778\times10^{-04}T^2 - 0.5001T + 324.29$$

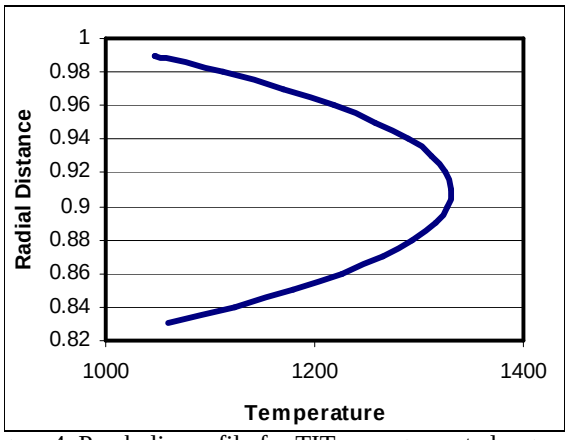

Figure 4. Parabolic profile for TIT arrangement along span height of nozzle

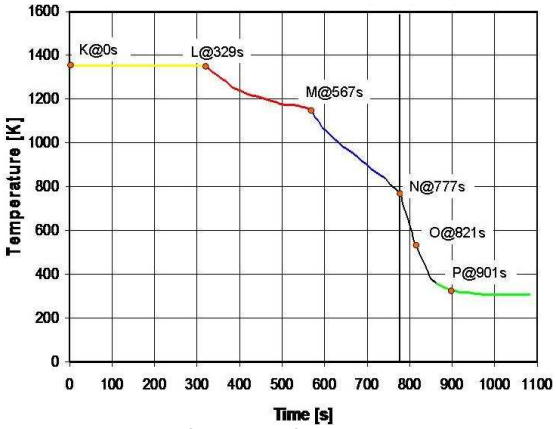

Figure 6. Points of analysis for temperature vs time during start-up curve.

Numerical parameters for unsteady

The calculation of each instantaneous solution can be seen as a pseudo-steady state problem, and one needs to determine the number of solver iterations required in order to reach convergence. Preliminary analyses have shown that higher numbers of solver iterations (or smaller time step sizes) were needed during the first phase of the process. The time step for each transient calculation of the Start-Up were set to $\Delta t = 7$ sec for (0 - 780 s interval), and $\Delta t = 15$s for (780-1024 s interval). For the Shut-down case the time steps were set to $\Delta t = 7$ sec during whole cycle.

It is important to notice that first iteration in the start-up cycle begun at 45 sec of start. That was due because from 0 to 45 sec of the start-up cycle were presented very high divergence because of low values in the BC´s, for that reason the process was simplified in order to have a good relation with computational costs.

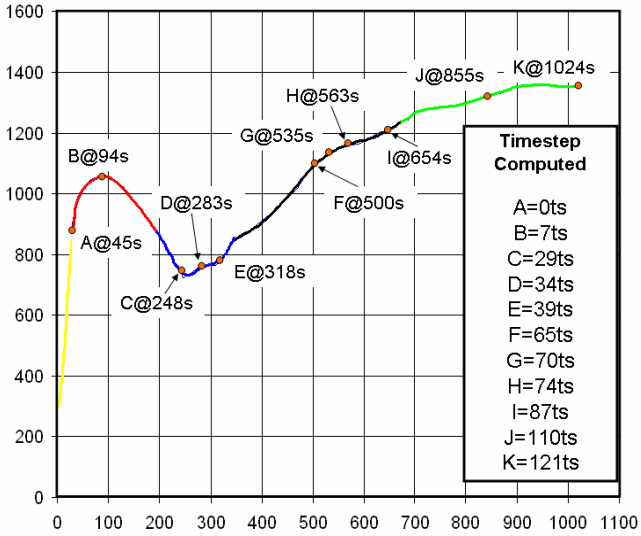

Figure 5. Points of analysis for temperature vs time during start-up curve.

Validation and Results

The results of the simulations are presented and analyzed in this section. For each cooling mass flow condition the heat transfer field was examined.

The validation of the model was made comparing the fluid parameters results at bucket outlet with turbine inter-stage parameter data test of gas turbine manufacturer. In table 4 are shown the main flow parameters results and the average errors obtained. From this results we can see that mean error is approximately 3.15 %, besides the turbulence model SA had a good convergence behavior with a total residual RMS = 4 and the error on mass flow prediction of 0.05%. The contours of temperature distribution at pressure side of Bucket have very good similitude with oxidation pots of bucket after 24,000 hours of operation. See Figure 7.

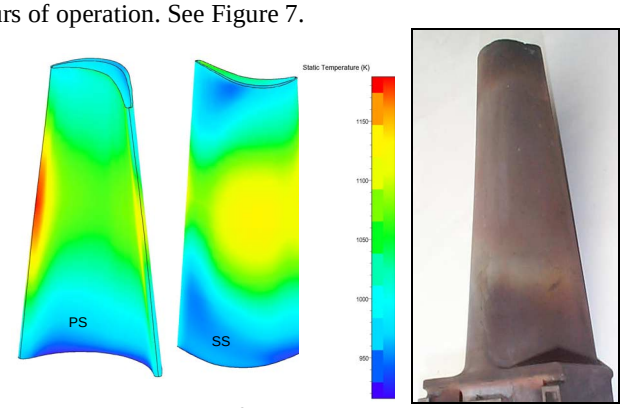

Figure 7. Contours of temperature distribution at pressure and suction sides in steady state simulation versus 24,000 hrs exposed bucket specimen.

Results and Discussion

The results were analyzed in eleven points of interest for Start-up and five points for the shut-down cycle.

Figure 8 shows the sequenced variations of calculated temperature distribution on coated bucket surface for each point of interest in both suction and pressure sides.

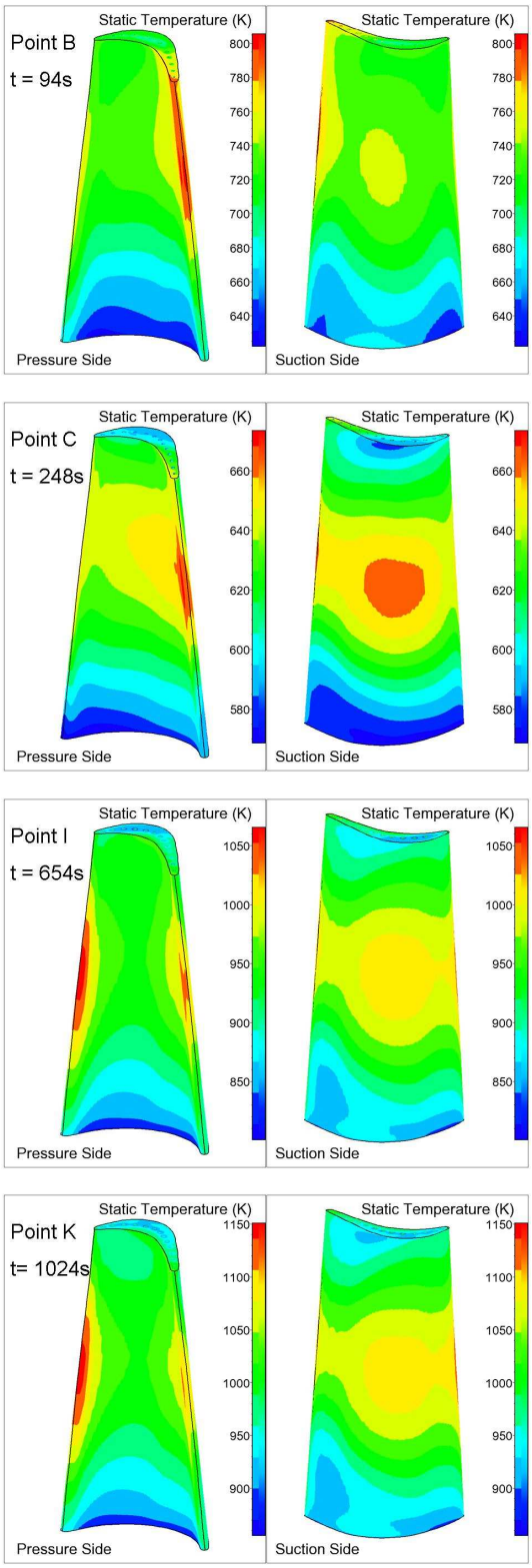

Figure 8. Temperature distribution sequence for points B, C, I and K of Start-up cycle.

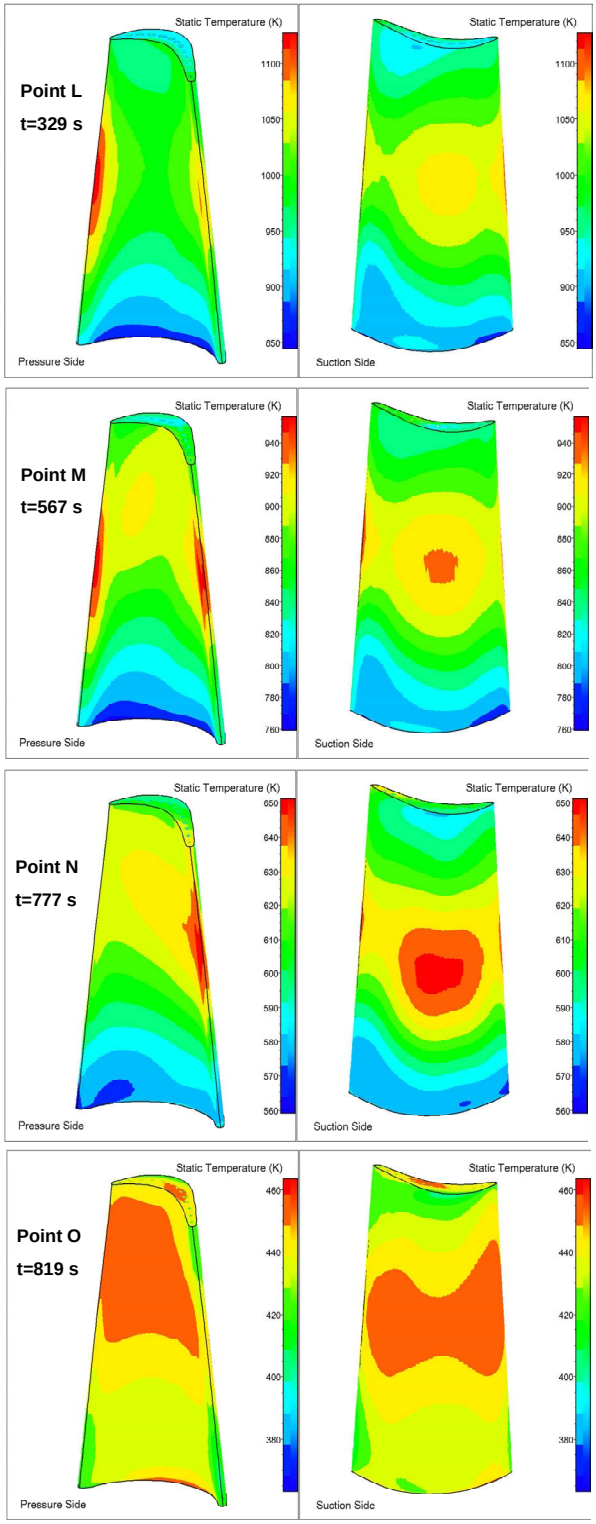

Figure 9. Temperature distribution sequence for points L, M, N and O of Shut-Down cycle.

Figure 8 shows the temperature distribution at different time steps, 94 sec, 248 sec, 654 sec and 1024 sec which represents the full load operation in the start-up cycle. Figure 9 shows the shut-down cycle temperature distribution at 329 sec, 777 sec and 819 sec.

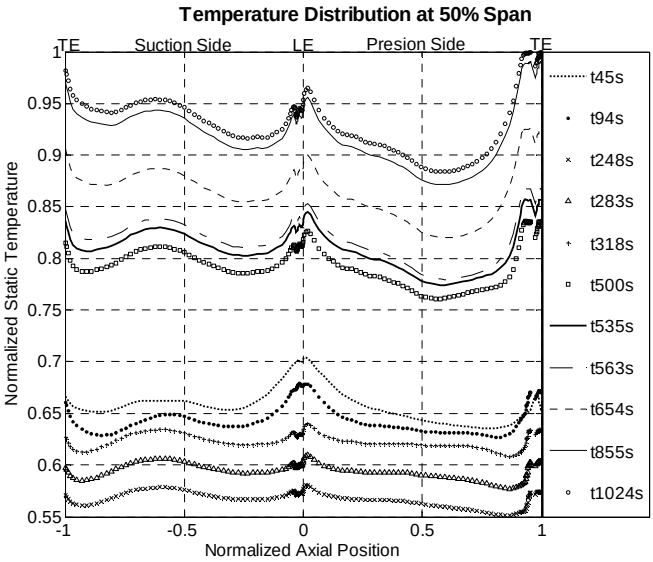

Figure 10. Bucket external surface base material normalized temperature distribution at different cross section during the whole start-up.

It can be appreciated that temperature distribution on blade external surface pattern during all start-up cycle is similar for S=0.5 blade section. It can be observed that at start-up initialization phase the temperature range on bucket suction and pressure sides are similar. At a later start-up cycle phase the temperature range on bucket suction side is higher than pressure side; the temperature plot in pressure side decreases (from LE to TE). This can be explained by the blade rotation effect making the heat transfer in suction side more important.

In order to analyze the effect of cooling holes during the start-up and shut-down cycle, the results were re-arranged to obtain the ΔT for base metal of bucket between blade external surface and cooling holes surface in a cross sectional view for 10%, 50% and 90% in spanwise locations.

Figure 11 illustrates the procedure used to obtain ΔT's in a cross section of bucket profile for each time step.

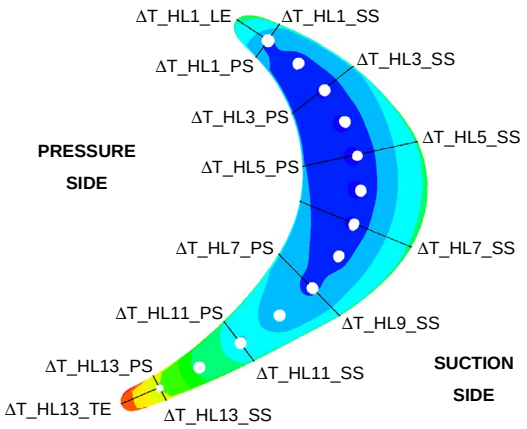

Figure 11. ΔT's sections used to sample maximum and minimum temperature between the cooling hole walls, and blade external surface.

Each ΔT_H represents the temperature difference between a cooling hole wall and the bucket surface at both suction and pressure sides for a given time step. To simplify data analysis only the 1, 3, 5, 7, 9 and 13 cooling hole positions were processed. Figure 12 shows the results of ΔT_H for bucket profiles at mid span cut during start-up cycle.

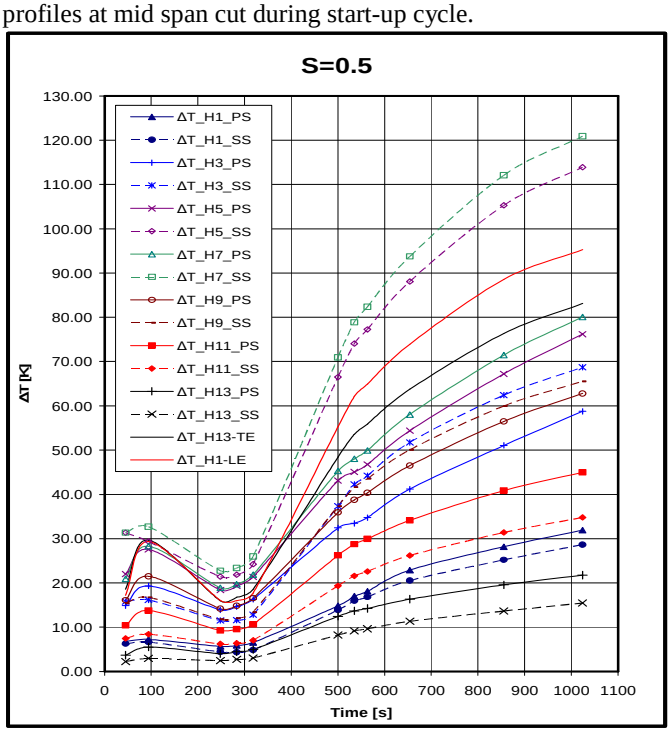

Figure 12. ΔT_H for bucket profiles at 50% spanwise for the start-up cycle.

It can be stated that temperature gradients variations between different reference points of the blade cross section is four times lower during start up initialization (point A) than that found during final phase of turbine start up cycle (point K). The maximum temperature gradients of the blade body during all start up cycle are registered invariable at central body of blade cross section, this zone correspond to cooling holes surfaces 5 and 7, and the blade external surface on the suction side. (See figure 12, ΔT_H7_SS, ΔT_H5_SS). This has relation with the blade wall thickness which is largest in this zone, thus generating the biggest temperature gradients. The leading edge (LE) and trailing edge (TE) zone follows in the second biggest temperature gradients. (Figure 12, ΔT_H1_LE, ΔT_H13_TE).

This behavior has direct relation with blade metal external surface temperature. The highest temperatures during all start up cycle are exhibited by LE and TE as can be appreciated in figure 10. It is important to notice that TE has highest surface temperature than LE surface, but has smaller temperature gradient. This can be explained because of the cooling hole in this zone (No.13) has the smallest diameter from all other cooling holes, and the smallest cooling flow. Therefore, related heat transfer generates a smaller temperature gradient than LE surface.

The smallest temperature gradients during all start up cycle are registered between cooling hole No. 13 and suction side (ΔT_H13_SS) of the blade surface, following cooling hole No. 13 and pressure side (ΔT_H13_PS); as well as cooling hole No. 1 in both suctions and pressure sides (ΔT_H1_SS, ΔT_H1_PS). See figure 12. These smallest temperature gradients distributions correspond to the blade smallest wall thickness.

From the results presented here it can be expected that maximum thermal stresses and related thermal fatigue cracks will be presented at the blade central section zone (cooling holes 5 to 7) and at LE and TE for start-up case.

In figure 13 are shown the same results than figure 12 but for shut-down case.

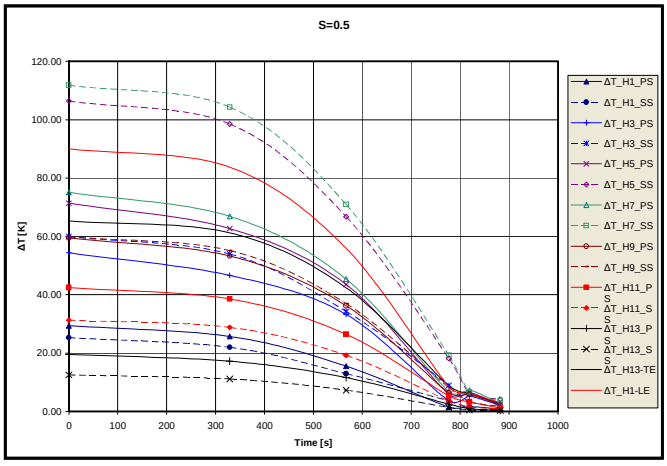

Figure 13. ΔT_H for bucket profiles at 50% spanwise for shut-down cycle.

From figure 13 it can be seen that major ΔT are also presented in suction side bucket body near to cooling holes 5 and 7 with a value that start from 112K. Then, section nearest to cooling hole number one follows as third highest ΔT with a initial value of 90 K on bucket cross-section. The minimum ΔT was for section near to cooling hole number 13 starting the shut-down with a value of 13K. The ΔT´s behavior for cross-section bucket metal are quite similar than start-up cycle.

The temperature distribution sequence for the Shut-down cycle in cross sectional view with S=0.5 are shown in figure 14.

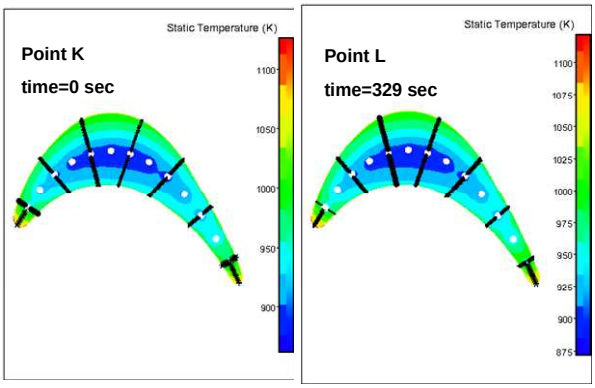

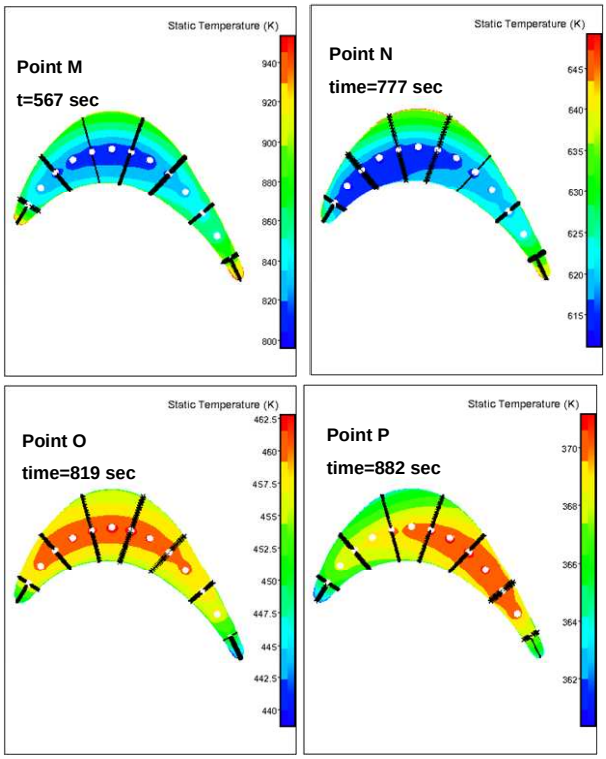

Figure 14. Temperature distribution sequence for the Shut-down cycle in cross sectional view with S=0.5.

The sequence shows the way of temperature distribution change in the cross sectional view of bucket profile during the shut-down cycle. The temperature becomes hotter in the internal body of bucket while shut-down time increases.

In the same way, ΔT's were obtained for the TBC behavior in cross sectional view of bucket profile at S = 0.5 for start-up case. (Figure 15).

From figure 15 it can be appreciated that TBC temperature gradients during start-up have similar behavior than inlet gas flow temperature during the same cycle. Besides the TBC gradients variation within bucket body during start-up initiation at different cooling holes zones are quite smaller than at final step of turbine start-up cycle. It means that TBC bucket protection is more effective at higher temperatures when main gas flow temperature and the cooling air flow temperature become stabilized.

The maximum temperature gradients during all start-up cycle are registered invariably between cooling hole surface No. 3 and suction surface profile (Fig. 15, ΔT_Coat_H3_SS). Besides, similar gradients levels are registered at hole No.1 zone (ΔT_Coat_H1_SS) which reaches slightly the highest value of at the final point of the start up cycle.

The maximum thermal stresses and maximum thermal fatigue cracks and coating spallation can be expected in this TBC zone.

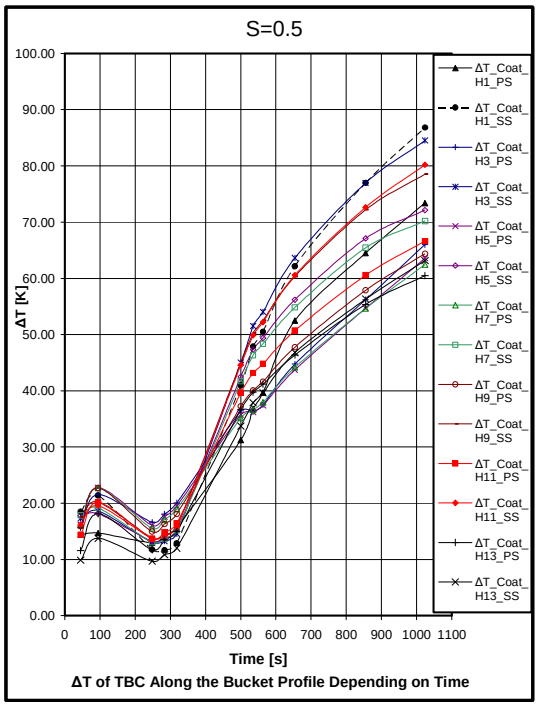

Figure 15. ΔT_H of TBC along the bucket profile at S=0.5 for the start-up cycle.

For the Shut-down case the ΔT's were also obtained for the TBC behavior in cross sectional view of bucket profile at S = 0.5 in figure 16.

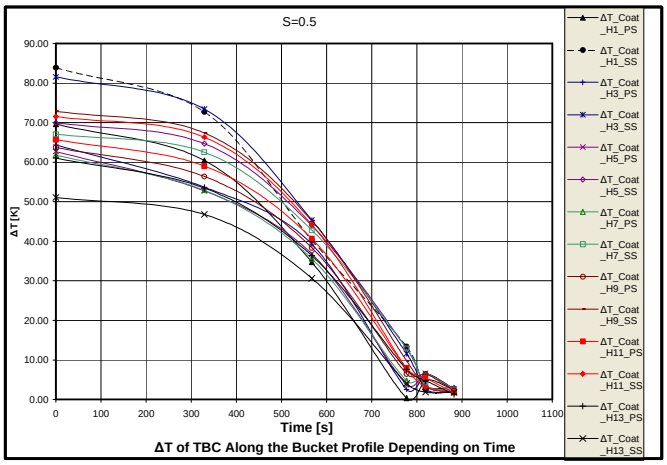

Figure 16. ΔT_H of TBC along the bucket profile at S=0.5 for the shut down cycle.

From figure 16 we can observe that the zone near to cooling hole number three shows the higher ΔT´s during whole shut-down cycles. Similar behavior presents the zone of cooling hole number one up to 300 sec., then shows a considerable decrease regarding cooling hole zone number three. The minimum value is shown in cooling hole number thirteen. The whole ΔT from TBC has similar behavior than main flow temperature during shut-down cycle.

SUMMARY AND CONCLUSIONS

The start-up and shut-down cycle was simulated using the characteristic diagrams of hot start-up cycle operation of a GT from Takahashi work [3] in order to predict the temperature distribution depending of time. The simulation of first stage stator-rotor includes the ejection of internal cooling air into gas path, meshing 13 internal cooling channels radially distributed along bucket body; the simulation also included meshing of a 0.4 mm thick YSZ-TBC. During all computation it was assumed a constant rotation of nominal speed, all other BC´s varied as a function of time and temperature.

The solver was able to compute the heat transfer of the blade bucket depending of variations of BC´s during the start-up and shut-down cycle simulation at an affordable computational cost.

The maximum temperature gradients of the blade body during all start up cycle were invariably registered at central zone of blade cross section. This zone corresponds to cooling holes surfaces 5 and 7 and the blade external surface on the suction side. (See figure 12, ΔT_H7_SS, and ΔT_H5_SS). This behavior was similar for shut-down case, showing maximum ΔT´s in zone of cooling holes number 5 to 7 at suction side. Figure 13.

The temperature gradients between TBC and bucket base surface metal in the same points of interest were analyzed. The maximum temperature gradients during all start-up and shut down cycle were registered invariably between cooling hole surface No. 3 and suction surface profile (Figure 15 ΔT_Coat_H3_SS). Besides, similar gradients levels were registered in hole zone No.1 (ΔT_Coat_H1_SS) which reach slightly the highest value at the final point of the start up cycle, having similarity. This indicates that main flow gas temperature behavior has a deep impact in the TBC ΔT during the whole cycle.

From previous results it is expected cracks initiation in cooling holes zones 5 to 7 of suction side, according with [8,9] investigation.

With these results it could be possible to estimate thermal stresses and residual life for the blade from the start-up and shut-down curve.

REFERENCES

[1] R. J. Boyle, "Effects of Thermal Barrier Coatings on Approaches to Turbine Blade Cooling" 2006, ASME paper GT-2006-91202.

[2] A Hernández-Rossette., Z. Mazur, et al. 2007, "Numerical 3D conjugated heat transfer simulation of a first inter-stage internal cooled thermal barrier coated gas turbine bucket, ASME POWER 2007 San Antonio TX, paper POWER 2007-22041.

[3] Takahashi T. and Watanabe K, 2001, "Transient Analyses of Conjugate Heat Transfer of a First Stage Rotor Blade in Start-Up and Shutdown", ASME Turbo Expo 2001, June 4-7, New Orleans, Louisiana, USA. ASME paper 97-GT-23.

[4] Numeca V.7.3 User´s Guide 2007.

[5] Launder B.E. and Spalding D.B., 1974, "The Numerical Computation of Turbulent Fluids", Comp. Meth, Appl. Mech. Eng. 3, pp.269-289.

[6] Jameson A. Baker, T. J., 1984, “Multigrid Solution of the Euler Equations for Aircraft Configurations”, AIAA Paper 84-0093
[7] York and Leylek, 2003, “Three-Dimensional Conjugate Heat Transfer Simulation of an Internally-Cooled Gas Turbine Vane”, ASME TurboExpo, Atlanta, Georgia, USA.
[8] Zdzislaw Mazur, Alberto Luna, Julio A. Juárez-Islas, 2005, “Metallurgical Assessment of Degradation of a Gas Turbine Bucket Made of Inconel 738LC Alloy After 24000 h In Service”, Proceedings of ASME POWER 2004, Baltimore, Maryland. PWR2004-52127.
[9] Zdzislaw Mazur, Alberto Luna-Ramirez, et al., 2005, “Failure Analysis of a Gas Turbine Blade made of Inconel 738 LC Alloy”, Journal of Engineering Failure Analysis, Elsevier, 12(2005) 474-486.
[10] Takahashi T., Watanabe K. and Takahashi T., 2000, “Thermal Conjugate Analysis of a First Stage Blade in a Gas Turbine”, ASME paper 2000-GT-251.
[11] Rigby D.L. and Lepicovsky J, 2001, “Conjugate Heat Transfer Analysis of Internally Cooled Configurations”, ASME Turbo Expo 2001, New Orleans, Louisiana, USA. ASME paper 2001-GT-0405.
[12] Zdzislaw Mazur, A. Hernandez-Rossette, et al., 2003, “Desarrollo de Herramientas para Predicción de Vida Útil Residual de Álabes de Turbinas de Gas” (in Spanish), Internal Report IIE/43/11887/I002/P/DI/A4, Electrical Research Institute, México. www.iie.org.mx.
[13]T. Fuji, T. Takahashi., 2004, “Development of operating temperature prediction method using thermophysical properties change of thermal barrier coatings”, Transactions of the ASME, Vol. 126.
[14] Kh. G Schmitt-Thomas and M. Hertter, 1991, “Improved oxidation resistance of thermal barrier coatings”, Surfaces and coating technology, 84-88, Elsevier.
[15] Zdzislaw Mazur, Alejandro Hernandez-Rossette, et al, 2005, “Analysis of conjugate heat transfer of a gas turbine first stage nozzle”, Asme Turbo expo 2005, Nevada, USA, Paper no. GT2005-68004
[16] Th. Hildebrant, J., M. Kluge Swoboda, et al. “Unsteady 3D Navier-Stokes calculation of a film cooled turbine stage: Part 2 – cooling flow modeling via discrete cooling holes”, European Commission, BRITE EURAM, Project contract No. BRPR-CT-0519, Project No. BE97-4440 (TATEF)
[17] Dieter E. Bohn and Christian Tummers, 2003, “Numerical 3-D conjugate flow and heat transfer investigation of a transonic convection-cooled thermal barrier coated turbine guide vane with reduced cooling fluid mass flow” ASME turbo Expo 2003, Atlanta Georgia, GT2003-38431.
[18] A. Demeulenaere, et al., 2005, “Application of an Unstructured Solver to the Calculation of Conjugated Heat Transfer Problems in Turbine Blades”, Proceedings of the European Turbomachinery Conference, Lille.
[19] Jameson, A., 1991, "Time dependent calculations using multigrid, with applications to unsteady flows past airfoils and wings", AIAA-Paper 91-1596.
[20] B. Tartinville, E. Lorrain, Ch. Hirsch, 2007, "Application of the V2F Model to Turbomachinery Configurations", ASME Paper GT2007-27708
[21] Bohn D.E., Becker V.J. and Kusterer K.A., 1997, “3D Conjugate Flow and Heat Transfer Calculations of a Film-cooled Turbine Guide Vane at Different Operation Conditions”, ASME paper 97-GT-23.

